Effect of eccentric location of rotating membranes in MBR

L. Sørensen*, T. R. Bentzen*

*Aalborg University, Department of Civil Engineering, Thomas Manns Vej 23, 9220 Aalborg Øst, Denmark

Summary:

In this work, it has been shown that an eccentric location of rotating membranes in a cylindrical tank has a positive effect regarding wall shear stresses compared to a concentric location. The study is made with CFD by use of a model that in a former study has been validated for a comparable setup. It has been shown that the rotation speed can be reduced with 33% to keep the same limiting flux with an eccentric location. As result of this, the energy consumption for the fouling mitigation can be lowered with 36% per m^3 of treated wastewater if the system is operated at limiting flux.

Keywords: CFD, rotating membranes, energy optimization, fouling mitigation

Introduction:

For wastewater treatment membrane bioreactors (MBR) has been manifested as a method that plays a larger and larger role [7]. One of the major drawback of the MBR is fouling of the membranes, resulting in a large energy consumption compared to conventional activated sludge treatment plants. It is generally agreed that the wall shear stresses on the membranes influence the tendency of membranes to foul. Higher wall shear stresses have a positive effect regarding antifouling of the membranes [5, 4] as well as fluctuations of the wall shear stresses which also help to reduce fouling [3]. One method for creating wall shear stresses is rotating membrane discs. Systems with rotating discs can be subdivided into setups with and without impellers. Where the setups can have, impellers rotating relative to the membranes to generate shear or without impellers where the rotation of the membranes generates the shear itself. This work treats such a setup, where the membranes are rotating to generate the shear. The geometry around the membranes will influence the flow and thereby have an impact of the wall shear stresses and makes this an obvious parameter for optimization.

Since measuring wall shear stresses is a very difficult task an obvious tool for the optimization is computational fluid dynamics (CFD). Different methods for modelling the rotating parts have been used in other studies. The moving reference frame was successfully used for a setup with impellers and water as the fluid [2]. In [11] the moving mesh method was successfully validated against LDA measurements of non-Newtonian fluid comparable to activated sludge. In this study, it was also concluded that the moving reference frame was less precise. The experimental setup used for this validation was based on the setup of Grundfos BioBooster. This work the same dimensions of the membranes and distance between them are used. The moving mesh method was also used in [9], for a setup with rotating impellers, where the results were successfully validated against measurements of wall shear stresses.

The CFD has been used for studying the effect of the locations of the membranes compared to the container. This is done my changing the location of the membranes on the x-axis illustrated on Figure 1.

For quantifying the positive effect of the different geometries, a relation between the limiting flux (J_{LIM}) and the energy consumption is found. Where the limiting flux is the maximum flux that can be achieved for the given condition where an increase in transmembrane pressure (TMP) will not increase the flux further. The experimental determination of the limiting flux is described in [6]. eq. 1 gives a relationship between wall shear stress (τ) and the limiting flux for a constant shear stress [5].

In that work the relationship was found for membranes with an average pore diameter of 60 nm in activated sludge.

$$J_{LIM} = 3.77 \cdot 10^{-5}\, \tau^{0.42}\, TSS^{\frac{1}{2}} \qquad \text{eq. 1}$$

Where TSS is the total suspended solids in kg/m^3.

The work needed to drive the shaft can be determined from the torque needed to rotate the membranes and the angle.

$$W = \int_{\theta_0}^{\theta_1} M \, d\theta \qquad \text{eq. 2}$$

And it follows that the power to drive the shaft at the rotational velocity ω can be expressed by eq. 3.

$$P = M\, \omega \qquad \text{eq. 3}$$

The relation between this limiting flux and the power needed to drive the membranes, can then be used to make an energy optimization. The efficiency of the motors at different working conditions is not included in this work.

Material and Methods:

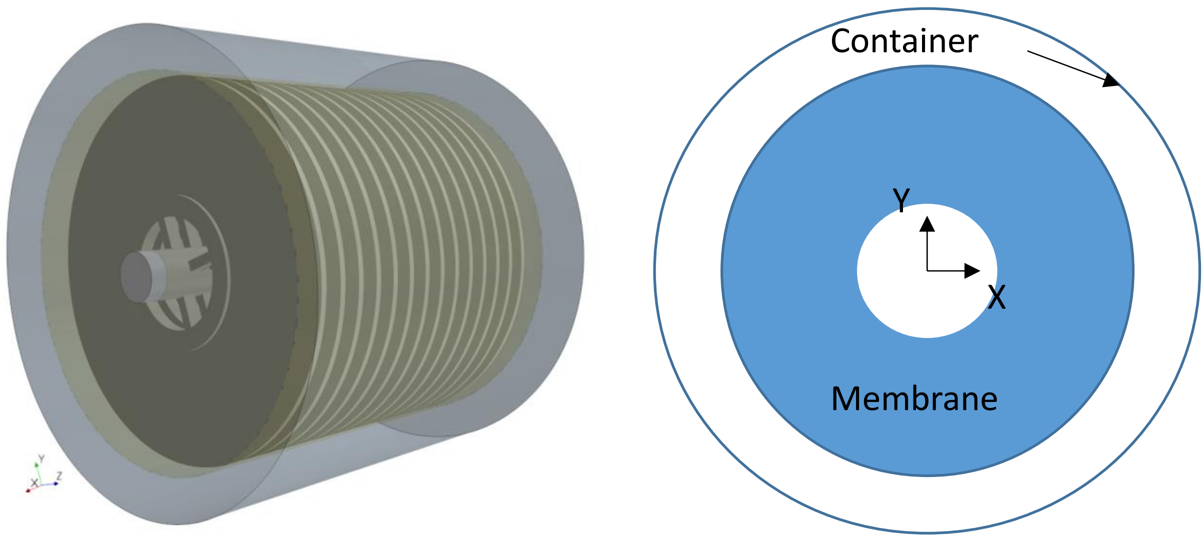

Figure 1 schematic setup of the membranes in the container.

The method for this study is CFD, which has previous been shown capable to model rotating membranes. The rigid body motion with a moving mesh is used, as it was shown in [11] that is was capable of modelling comparable setups, concerning both the geometries and the rotation rates. In that study the model was validated against rotation rates of 120 RPM, with both a concentric and an eccentric location of the membranes in a quadratic box. The liquid used in the experiments was CMC solutions, which has shear thinning properties like activated sludge. The rigid body motion is a transient method allowing the actual motion of the geometry. The continuum is split into two regions connected by an interface, where the velocities are translated from the one mesh to the other. The inner region containing the membranes is set to have a constant rotation rate, while the region outside is set to be fixed.

The setup is made in accordance to industrial available MBR setups with rotating membranes, where Grundfos BioBooster has a setup working with this eccentric location. The system is non-aerated and is therefore modelled as a single-phase system, where eventual particles are neglected. Furthermore, the filtration from the membranes is neglected, meaning that there is a zero-velocity normal to the membrane surface.

The geometry of the membranes corresponds to the one used for validation of the model in [11] with membranes with an inner diameter of 151 mm and an outer diameter of 374 mm, while the container has a diameter of 457 mm. For the concentric setup, this leaves a gap of 41.5 mm between the tip of the membranes and the container. For the eccentric setup, the container was moved 20 mm in the x direction, leaving a gap of minimum 21.5 mm and maximum of 61.5 mm between the membranes and the container. The distance between the membranes is 17.9mm. The rotation rates of the membranes were varied in the range from 80 RPM to 120 RPM. The interface between the two regions is in a radial distance of 190 mm from the rotation center.

The rheology of the fluid is described with the power law as $\mu = 1.298\, \dot{\gamma}^{0.278-1} Pa\, s$, corresponding to a MBR sludge concentration of 22.5 gTSS/l [10], where comparable setups operates at concentrations in the range 0 and 40 gMLSS/l [1], where MLSS is the mixed liquor suspended solids.

The flow is modelled as laminar in accordance to [11] where this was shown to be valid. In [5, 8] the non-Newtonian Reynolds number in rotating systems was calculated from eq. 4 and the flow was assumed laminar if under 45000. With a rotation rate of 120 RPM and a kinematic viscosity ν of $0.197 \cdot 10^{-3}$ m^2/s which was the volume averaged kinematic viscosity in the concentric model, eq. 4 results in a Reynolds number of 2230 at the tip of the membranes. This substantiates the assumption of a laminar flow.

$$Re = \Omega_{\mathrm{rad}} r^2 / \nu \qquad \text{eq. 4}$$

Where, Ω_{rad} is rotation rate in rad/s and r is the radius.

Table 1 moment on single membrane for difference meshes for the concentric setup.

NUMBER OF CELLS	MOMENTS [NM]
$0.99 \cdot 10^6$	0.426
$3.31 \cdot 10^6$	0.426
$5.24 \cdot 10^6$	0.421

The mesh is made with the polyhedral mesher in STAR CCM+ and with use of thin prism layers at the walls. The meshes of the two regions are connected at the interface. A mesh dependency test was made, where the results are shown in Table 1. Due to the very small difference on torque in the setups, the cell sizes resulting in $3.31 \cdot 10^6$ cells are used for all setups.

Results and discussions:

The comparison of the results is made with two different rotational velocities. The concentric setup is with a rotation rate of 120 RPM and the eccentric setup with a rotation rate of 80 RPM. The different rotations rates are chosen as the eccentric setup resulted in significantly higher shear stresses than for the concentric setup and thereby also an increased moment needed to rotate the membranes. For the determination of the moment, both the contribution from the pressure and the shear are included. For one side of a single membrane, the moment was 0.064 Nm for the eccentric setup compared to 0.0424 Nm for the concentric setup. With the rotation rate of 80 RPM the moment was reduced to 0.0446 Nm and thereby comparable to the concentric setup. A snapshot of wall shear stresses for these two setups is shown in Figure 2. The concentric setup has increasing wall shear stresses with increasing radii with some dead zones. For the eccentric setup, the membrane is split into two parts, where the left part has lower wall shear stresses than the right side of the membrane. On the right side with the high shear stresses it is clear that they are presented even at a low radii minimising the risk of fouling in that area contradictory to the concentric setup. Another important factor which can be seen from Figure 2 is size of the areas of high and low wall shear stresses, where there are three small areas of each for the concentric setup, there is one large zone of each for the eccentric setup. It has been shown that a long duration of high wall shear stresses are more effective for fouling control than shorter but more frequent periods of high shear [3], favorising the eccentric setup.

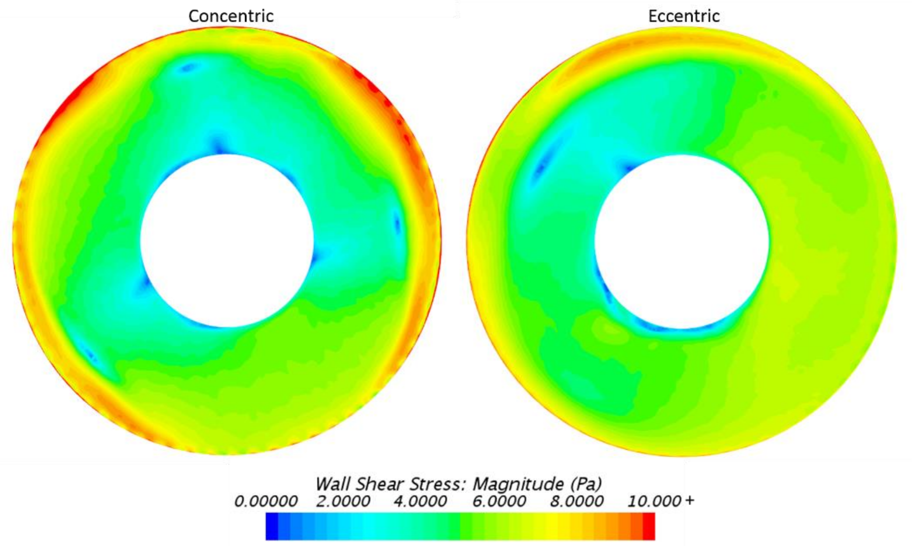

Figure 2 snapshot of wall shear stresses at single membrane for concentric and eccentric setup.

To make a quantitative comparison between the two setups, the wall shear stresses have been extracted at different radial locations on the surface of a single membrane. The data points are located a at fixed radius from 90 to 170 mm from the rotation center and set to follow the motion of the membranes. Data is then extracted for a period corresponding to 5 rotations of the membrane, which is 2.5 seconds for the concentric setup and 3.75 seconds for the eccentric setup. Examples of these time series for three different radii is illustrated in Figure 3. It can be seen, that even though the setup is completely concentric, there are still some fluctuations.

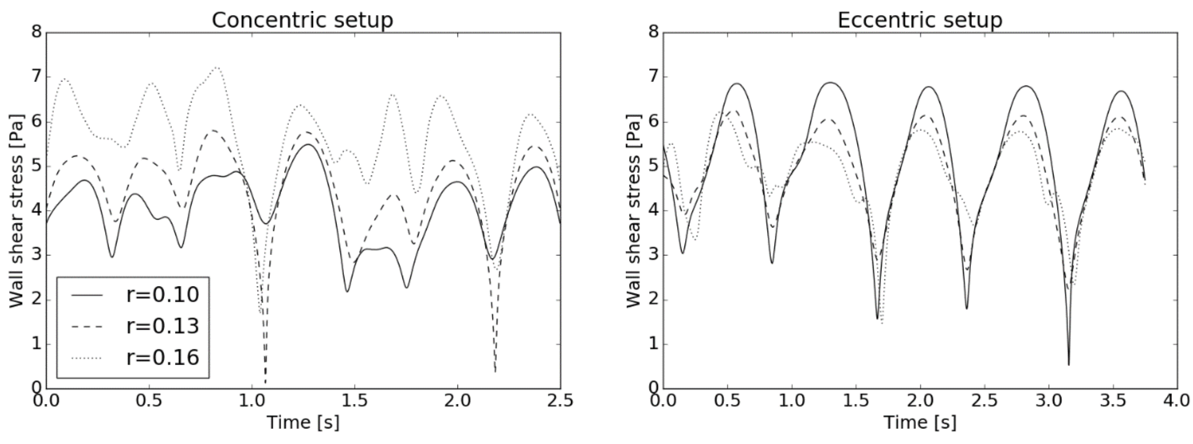

Figure 3 time series for wall shear stress in different radii (r).

The data from the time series is used for making the statistics to be able to compare the two setups. It is found the mean wall shear stresses for the most points are higher for the eccentric setup than for the concentric setup illustrated in Figure 4 A). Another thing that is important to notice is the way the wall shear stresses are distributed. In the eccentric setup, there is a more even distribution of wall shear stresses as function of radii compared to the concentric setup. This is positive since the antifouling effect is much more evenly distributed. Where the concentric setup has a stronger tendency of increasing wall shear stresses as function of radius.

In Figure 4 b) the maximum values of the wall shear stresses are shown. These results show the same positive effect as the mean wall shear stresses, where the maximum wall shear stresses are more evenly distributed resulting in a more even antifouling effect of the entire membrane.

The standard deviation of the wall shear stresses is shown in Figure 4 c) as it has been found that there is a relationship between the standard deviation of the wall shear stresses and the fouling rate [3]. Here it can be seen that the standard deviation on the wall shear stresses in most points are higher for the eccentric setup favorizing this setup.

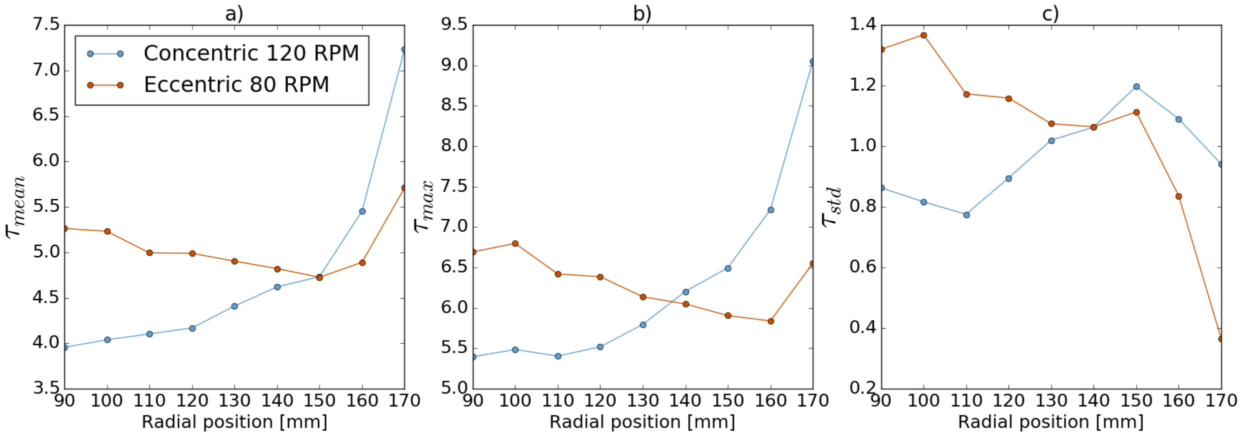

Figure 4, a) mean wall shear stresses, b) maximum wall shear stresses and c) standard deviation of wall shear stresses at the membrane surface in different radii.

To get a direct measure of the effect of the eccentricity a comparison between limiting flux and energy consumption is made. The limiting flux into the membranes is determined from eq. 1 with use of instantaneous wall shear stress. This is integrated up over the entire area of all the membranes. Again, the time series of 5 rotations is used and the mean flux over this period is determined. The energy consumption is calculated from the moment and the rotational velocity. The moment is exported for the entire rotating part of the system since it will all contribute to the energy consumption. With the exported moment, the power is determined from eq. 3. The results of energy and flux are listed in Table 2. The efficiency for fouling mitigation is improved significantly with the eccentric setup, where only 63% of the energy is needed for the fouling mitigation for the same amount of treated wastewater when operated at limiting flux.

Table 2, power, limiting flux and efficiency of fouling mitigation when operated at limiting flux.

	POWER [W]	J_{LIM} [M^3/H]	EFFICIENCY OF FOULING MITIGATION [KWH/M^3]
CONCENTRIC	20.0	0.146	0.135
ECCENTRIC	12.7	0.149	0.085

- The study showed that it is possible to achieve the same limiting flux, with use of 37% less energy with use of relationships for steady shear by use of an eccentric location of the membranes compared to a concentric location.
- The study showed that an eccentric location of the membranes gives larger standard deviations, longer duration of fluctuations and higher maximum wall shear stresses, which all have been shown to have a positive effect on minimizing fouling.

Bibliography

[1] Grundfos Biobooster a/s. Next-generation wastewater treatment, 2013.

[2] Thomas Ruby Bentzen, N Ratkovich, S Madsen, JC Jensen, SN Bak, and Michael R Rasmussen. Analytical and numerical modelling of newtonian and non-newtonian liquid in a rotational cross-flow mbr. *Water Science and Technology*, 66(11):2318–2327, 2012.

[3] CCV Chan, PR Bérubé, and ER Hall. Relationship between types of surface shear stress profiles and membrane fouling. *Water research*, 45(19):6403–6416, 2011.

[4] Michel Y Jaffrin, Lu-Hui Ding, Omar Akoum, and Ambroise Brou. A hydrodynamic comparison between rotating disk and vibratory dynamic filtration systems. *Journal of Membrane Science*, 242(1):155–167, 2004.

[5] Mads K Jørgensen, Malene T Pedersen, Morten L Christensen, and Thomas R Bentzen. Dependence of shear and concentration on fouling in a membrane bioreactor with rotating membrane discs. *AIChE Journal*, 60(2):706–715, 2014.

[6] Mads Koustrup Jørgensen, Thomas Vistisen Bugge, Morten Lykkegaard Christensen, and Kristian Keiding. Modeling approach to determine cake buildup and compression in a high-shear membrane bioreactor. *Journal of membrane science*, 409:335–345, 2012.

[7] Simon Judd. *The MBR book: principles and applications of membrane bioreactors for water and wastewater treatment*. Elsevier, 2010.

[8] Ali A Rashaida. *Flow of a non-Newtonian Bingham plastic fluid over a rotating disk*. PhD thesis, 2005.

[9] N Ratkovich, CCV Chan, Thomas Ruby Bentzen, and Michael R Rasmussen. Experimental and cfd simulation studies of wall shear stress for different impeller configurations and mbr activated sludge. *Water Science and Technology*, 65(11):2061–2070, 2012.

[10] Sandra Rosenberger, Kirsten Kubin, and Matthias Kraume. Rheology of activated sludge in membrane bioreactors. *Engineering in life sciences*, 2(9):269–275, 2002.

[11] Lasse Sørensen, Thomas Ruby Bentzen, and Kristian Skov. Validation of computational non-newtonian fluid model for membrane bioreactor. *Water Science and Technology*, 72(10):1810–1816, 2015.